RSC Advances

ROYAL SOCIETY OF CHEMISTRY

www.rsc.org/advances

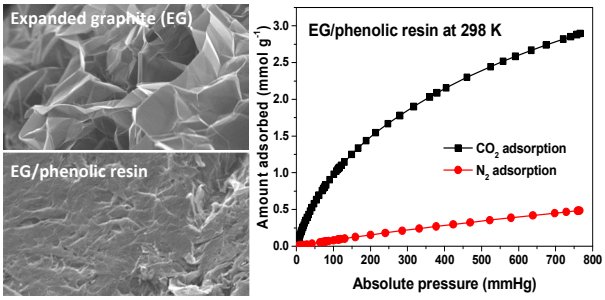

Incorporating a small proportion of expanded graphite dramatically improves microporosity and CO_2 uptake of phenolic resin-derived activated carbons.

Expanded graphite/phenolic resin-based carbon composite adsorbents for post-combustion CO_2 capture†

Yonggang Jin, *[a] Chi P. Huynh,[b] Stephen C. Hawkins[c,d] and Shi Su*[a]

[a]CSIRO Energy Flagship, PO Box 883, Kenmore, Qld 4069, Australia

[b]CSIRO Manufacturing Flagship, PMB 10, Clayton, Victoria 3168, Australia

[c]School of Mechanical and Aerospace Engineering, Queen's University Belfast, Belfast, BT9 5AH, UK

[d]Department of Materials Engineering, Monash University, Clayton, Victoria 3800, Australia

*Correspondence authors:

Email: yonggang.jin@csiro.au; Tel: +61-7-33274146; Fax: +61-7-33274455

Email: shi.su@csiro.au; Tel: +61-7-33274679; Fax: +61-7-33274455

† Electronic supplementary information (ESI) available.

Abstract

Porous carbon composite adsorbents were prepared from a commercial phenolic resin mixed with a small proportion of thermally expanded graphite (EG) followed by carbonization and physical activation with CO_2. The addition of EG dramatically hastens the CO_2 activation and results in remarkably enhanced microporosity development in the EG composite compared to the activated phenolic resin alone. The resultant EG composite adsorbents exhibit high CO_2 adsorption capacities at 298 K and excellent CO_2/N_2 adsorption selectivity. In particular, the EG composite shows superior CO_2 uptake at low CO_2 pressures (47 mg g^{-1} at 298 K and 0.15 bar), which is more important to actual flue gas applications in post-combustion capture (PCC). Moreover, EG composite adsorbents are especially attractive as the EG component is inexpensive, available in very large amounts and easy to handle and is only required at a low addition level of around 2 wt%. The rapid CO_2 activation and the low burn-off for excellent CO_2 adsorption performance at low pressures greatly reduce the energy required to produce the adsorbent and the waste generated in activation. This further enhances the cost and environmental advantages of physically activated EG composites over those PCC adsorbents prepared by chemical activation and functionalization of porous carbons. Hence, due to its superior CO_2 adsorption properties and favourable fabrication process, the newly developed EG carbon composite adsorbent holds great promise for large-scale deployment and commercial applications to PCC.

Keyword: Porous carbon, Phenolic resin, Expanded graphite, Physical activation, CO_2 capture

1. Introduction

Growing concern with human-induced climate change has attracted widespread efforts to develop cost-effective and robust technologies for post-combustion capture (PCC) of carbon dioxide (CO_2) from large point sources such as coal-fired power stations.[1] The PCC of CO_2 with solid adsorbents is considered a promising alternative to the conventional solvent process which uses chemical absorption with aqueous amine solvents.[2,3] Although this is currently the most commercially available PCC technology, the solvent process is energy-intensive and requires strict pre-cleaning treatments to the flue gas. Moreover, it raises environmental concerns due to large volumes of waste water and sludge produced from the solvent process and secondary emissions resulted from the solvent degradation. By contrast, the solid adsorbent process is a low-energy and environmentally-benign technology. It is based on simple physisorption of CO_2 with lower heat of CO_2 adsorption compared to chemical absorption, which implies potentially lower energy consumption needed for CO_2 desorption in adsorbent regeneration. As solid adsorbents are thermally stable and chemically non-reactive with CO_2 adsorbates, there are no environmental impacts due to degradation in the adsorbent process. If solid adsorbents are also tolerant of impurities (i.e. SO_x and NO_x) in the flue gas stream, significant savings in the overall capture cost could be made by removal of flue gas pre-treatments.

A large number of solid porous materials have been investigated for CO_2 capture including zeolites, porous carbons, functionalized porous silica, metal-organic frameworks and covalent organic frameworks.[4-13] Carbonaceous adsorbents have advantages such as low cost and high chemical, thermal and mechanical stability necessary to operate in realistic flue gas streams. However, they generally have poor CO_2 adsorption capacity, which reduces their cost-effectiveness because more adsorbents are needed to cope with a given flue gas flow and more energy is required to achieve regeneration because more sensible heat is required to heat up a larger amount of adsorbents for thermal regeneration.

Approaches to improving the CO_2 adsorption capacity of carbonaceous materials have been mainly focused on (1) development of high-surface-area microporous carbons in a chemical activation method by blending carbon precursors with a very large proportion of harsh chemicals such as KOH followed by pyrolysis;[10,14,15] and (2) functionalization of porous carbons with basic groups, such as nitrogen doping and amine loading.[16,17] Although CO_2 adsorption capacity is improved, there is a high complexity, cost, waste and inconvenience with chemical activation as large amounts of hazardous chemicals are used and chemical residues have to be thoroughly washed out. The functionalization method also has greater complexity or cost, and some functionalized carbons show difficult and unstable regeneration due to strong interactions with CO_2.

The CO_2 adsorption capacity of porous carbons can also be improved by physical activation, which entails etching carbons with mild oxidant gases such as CO_2 and steam at elevated temperatures, a process that is much more economically and environmentally attractive than chemical activation.[18] An important issue with physical activation, particularly for carbon monoliths desirable for practical applications, is mass transport/diffusion of the etchant gases during oxidation.[19] Facilitated mass transport of oxidizing molecules within the carbon structure is requisite to boost the reaction of physical activation, thereby enhancing the development of the narrow microporous structure in physically activated carbons for improved CO_2 adsorption at ambient conditions.

We recently reported the preparation of carbon composite monoliths with exceptional CO_2 adsorption capacity and kinetics, and excellent CO_2/N_2 selectivity.[20] It used a commercial phenolic resin mixed with just 1 wt% of carbon nanotubes (CNTs) and physical activation with CO_2. The outstanding performance is attributed to the monolith possessing a hierarchical macroporous-microporous structure with a very high proportion of narrow micropores. The proposed formation mechanism is that the CNTs act as a nanoscale scaffold to establish a macroporous structure in the resin-derived carbon after carbonization, which allows easy access of activating agent CO_2 molecules to the monolith's interior.

The CNTs also offer a large primary surface area by distributing the resin-derived carbon into micro/nanometre scale domains, thus providing more locations for rapidly creating a large population of narrow micropores in the course of CO_2 activation. As a result, the CO_2 activation for the CNT-incorporated composite is remarkably quick, exhibiting much greater burn-off than the phenolic resin alone derived carbon at a given period of time and the rapid activation also minimizes pore widening. Therefore, it can be seen that fast mass transport of activating agent molecules is very important to the development of an optimum microporous structure in physically-activated carbons.

In the present study, we incorporated expanded graphite (EG) into phenolic resins to produce carbon composite adsorbents by physical activation with CO_2. Compared to CNTs, EG is of lower cost, and easier to make, handle and disperse in the preparation of composites. The large surface area and high aspect ratio (platelet diameter to thickness) of EG is anticipated to function in a somewhat similar manner to CNTs for achieving well-developed narrow microporous structures in the EG/phenolic resin-based carbon composite. The resultant EG monoliths were characterized for surface morphologies, pore structures and gas adsorption properties to understand the effects of EG addition on the development of microporous structures in phenolic resin derived activated carbons as well as to evaluate CO_2 capture performance of EG composites for PCC.

2. Experimental

EG was prepared from commercial expandable graphite flakes (Asbury Carbons, Grade 3772, 80% >300 µm and carbon content 99%). The expandable graphite flakes were thermally expanded and exfoliated by heating 3 g batches in loosely capped 500 ml single-use tin cans at 1050 ^{o}C in a muffle furnace for 3 min. This amount produced approximately 2.5 g of EG which is sufficient to fill the can, which was allowed to cool before opening. The obtained EG powders were well dispersed in an

aqueous gel solution containing 5 wt% of methyl cellulose (MC, Aldrich, viscosity (2% in H_2O) = 4,000 cp).

EG carbon composites were prepared by thoroughly mixing 5 g of commercial Novolac phenolic resin (Durez 7716) powder with a given amount of the EG gel paste. The resultant highly viscous mixture was transferred into a cylindrical polypropylene mold (20 mm inner diameter) with five 2 mm diameter channel pins, and then cured at 150 ^oC for 2 h to solidify the structure. After de-molding, the honeycomb monolith with five channels was carbonized in a tube furnace at 650 ^oC for 1 h under N_2 flow. The carbonized sample was weighted, returned to the tube furnace and heated to 950 ^oC under N_2 flow. At the setpoint temperature, the gas flow was switched to CO_2 for a given period to activate the sample with CO_2, and then back to N_2 as the sample was cooled. The activated sample was weighed to determine the burn-off (defined as ((mass of carbonized sample - mass of activated sample)/mass of carbonized sample) x 100%)) during activation. The activated EG composites were labeled as EG-x-y, where x = the % EG to resin (i.e. mass percentage of EG/phenolic resin) with values of 2, 5 and 10 %, and y = the activation time with values of 15 and 30 min. For comparison, the activated sample made of phenolic resin alone without EG was prepared and labeled as Res-60, denoting 60 min activation time.

Sorption measurements for N_2 and CO_2 were carried out on Micrometritics ASAP 2020 volumetric analyzer at various temperatures after degassing overnight under vacuum at 473 K. The Brunauer-Emmett-Teller (BET) specific surface area (S_{BET}) and the total pore volume (V_t) were obtained from N_2 adsorption isotherms at 77 K. S_{BET} calculation was performed below 0.1 relative pressure and V_t was calculated by the N_2 amount adsorbed at the relative pressure of about 0.99. Adsorption isotherms for CO_2 at 273 K were used to obtain the narrow micropore (< 1 nm) size distributions, which were calculated by the density function theory (DFT) method. The surface area (S_{nm}) and the volume (V_{nm}) of narrow micropores were derived from the above calculations. For comparison, the DFT calculation

was also conducted on the N_2 adsorption isotherm at 77 K to determine the NMPSD. The heat of CO_2 adsorption was calculated using CO_2 isotherms at 273, 298 and 323 K based on the Clausius-Clapeyron equation. Morphologies of samples were examined using scanning electron microscopy (SEM, Nava Nano SEM 430) at an operating voltage of 5 kV. The SEM observation was conducted on the sample without coating. Transmission electron microscopy (TEM) was performed on a Tecnai T12 at an operating voltage of 120 kV.

3. Results and discussion

Prior to thermal treatment, the expandable graphite shows a bulky micro-morphology composed of dense graphite flakes (Fig. 1a). Its specified expansion ratio is 270 ml g^{-1} minimum; however if allowed to expand to this extent, the material is intolerably fluffy and difficult to work with. Thus samples were constrained to a density of 2.5 g to 500 ml or 200 ml g^{-1}. The obtained EG is nevertheless very fluffy and appears in a worm-like particulate shape. As shown in Fig. 1b, EG exhibits an irregular porous network comprising a mass of graphite nanosheets separated by voids and crevices of micron to nanometer. Such morphology is resulted from exfoliation and distortion of graphite nanosheets during rapid thermal expansion and consistent with the observation reported previously.[21] The BET surface area (S_{BET}), obtained from N_2 adsorption isotherms at 77 K (ESI Fig. S1), increases from 0.9 m^2 g^{-1} for the expandable graphite to 34.3 m^2 g^{-1} for the EG. In addition, the N_2 isotherm of the EG shows a hysteresis loop at relative pressures above 0.5, indicating the presence of mesopores.

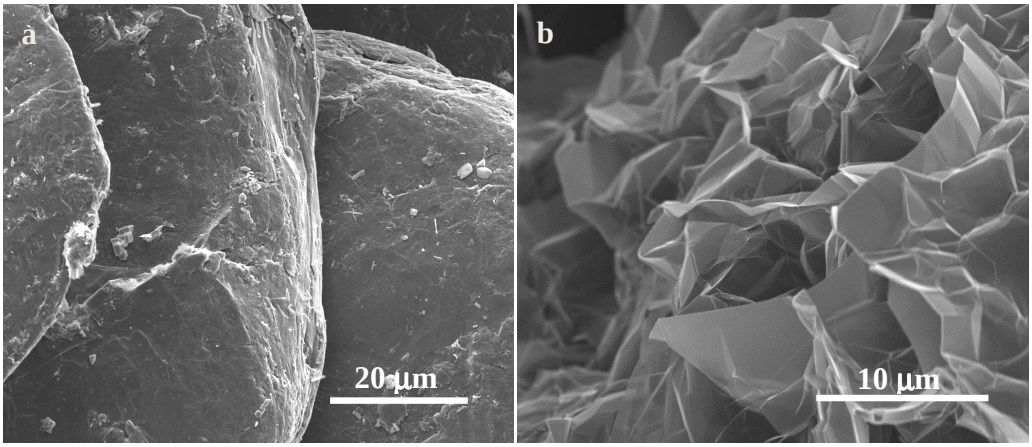

Fig. 1 SEM images of (a) the expandable graphite and (b) the expanded graphite (EG).

The surface morphologies of the activated phenolic resin and the EG composite were analyzed by SEM which reveals a dramatic difference after incorporating EG (Fig. 2 a-c). The resin alone derived Res-60 exhibits a bulky and dense structure with large vapor holes and little secondary structure such as pores and channels (Fig. 2a). By contrast, the EG composite (EG-5-30) presents a porous microstructure composed of interconnected irregular large particles and shows porosity and channeling at a range of scales from sub-millimeter down (Fig. 2 b,c). The original porous network of the EG is covered with resin derived carbons in the EG composite (Fig. 2c), which splits the phenolic resin and subsequently the derived carbon (after carbonization) into small domains that would contribute to the rapid and uniform development of micropores in CO_2 activation. The TEM image of the EG composite, as shown in Fig. 2d displays the disordered micropores distributed all over the carbon material, which are responsible for CO_2 adsorption under ambient conditions.

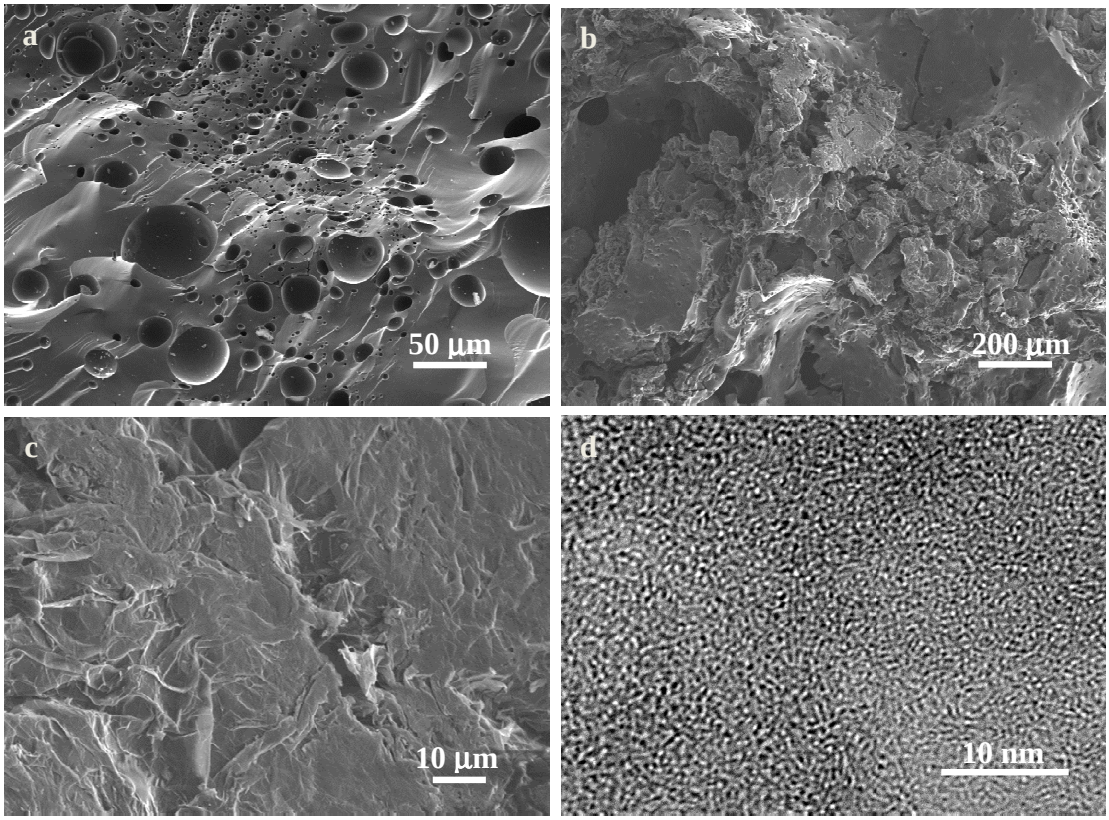

Fig. 2 SEM images of (a) the activated phenolic resin Res-60 and (b,c) the EG composite EG-5-30 at different magnifications, and (d) TEM image of EG-5-30.

It can be seen from Table 1 that the composites with EG incorporated are much more reactive with CO_2 during activation, exhibiting significant burn-off within much shorter activation duration. Although 7.6 wt% of burn-off was achieved in resin alone derived Res-60 when activated at 950 ^{o}C for 60 min, the EG composites took just 30 min to reach the levels of burn-off 2 to 4 times higher. The more EG was incorporated, the higher burn-off was achieved. When the EG composites were activated at 950 ^{o}C for 30 min, the burn-off reached 14.3 wt% for EG-2-30, went up to 19.9 wt% for EG-5-30 and doubled to 27.4 wt% for EG-10-30. The dramatic increase of burn-off with the inclusion of EG is likely attributed to the EG's modifications to the microstructure of phenolic resin derived carbons. As discussed above,

in contrast to resin alone Res-60, the EG composite has a porous microstructure which would favor mass transport of activating agent CO_2 within the monolith, thus leading to rapid burn-off.

Table 1 Burn-off, textual properties and CO_2 adsorption capacities of activated adsorbents

Samples	Burn-off	N_2 adsorption at 77K		CO_2 adsorption at 273K		CO_2 uptake at 298 K (mg g^{-1})	
	(wt%)	S_{BET} (m^2 g^{-1})	V_t (cm^3 g^{-1})	S_{nm} (m^2 g^{-1})	V_{nm} (cm^3 g^{-1})	1 bar, C_{100}	0.15 bar, C_{15}
Res-60	7.6	237	0.108	317	0.092	82	24
EG-2-30	14.3	723	0.290	527	0.157	135	45
EG-5-30	19.9	908	0.367	477	0.143	128	40
EG-10-30	27.4	1028	0.439	413	0.125	113	33
EG-2-15	7.6	523	0.205	542	0.159	127	47

To study the effects of EG addition on the textual properties, N_2 and CO_2 sorption measurements were carried out at 77 and 273 K, respectively. Fig. 3a shows N_2 adsorption-desorption isotherms for the activated phenolic resin (Res-60) and three EG composites activated for 30 min. All the isotherms display significant steep N_2 uptake at low relative pressures followed by an adsorption plateau, typical for microporous materials.[22] A slight hysteresis for EG-10-30 at relative pressures above 0.5 is similar to the N_2 sorption behavior of pure EG (ESI Fig. S1), suggesting that the EG content in this sample may be excessive and some has failed to disperse effectively. As seen from Table 1, the EG composites exhibit a significantly enhanced porous structure compared to resin alone derived Res-60. The surface area S_{BET} is 237 m^2 g^{-1} for Res-60 and dramatically increased to 723 m^2 g^{-1} for EG-2-30. With more EG incorporated, S_{BET} is increased to 908 m^2 g^{-1} for EG-5-30 and further to 1028 m^2 g^{-1} for EG-10-30. Similarly, pore volumes (V_t) of the composites are remarkably higher than Res-60, and V_t is increased as the addition amount of EG is increased. Therefore, the results clearly indicate that the incorporation of EG greatly enhances the development of microporous structures in the phenolic resin derived carbons.

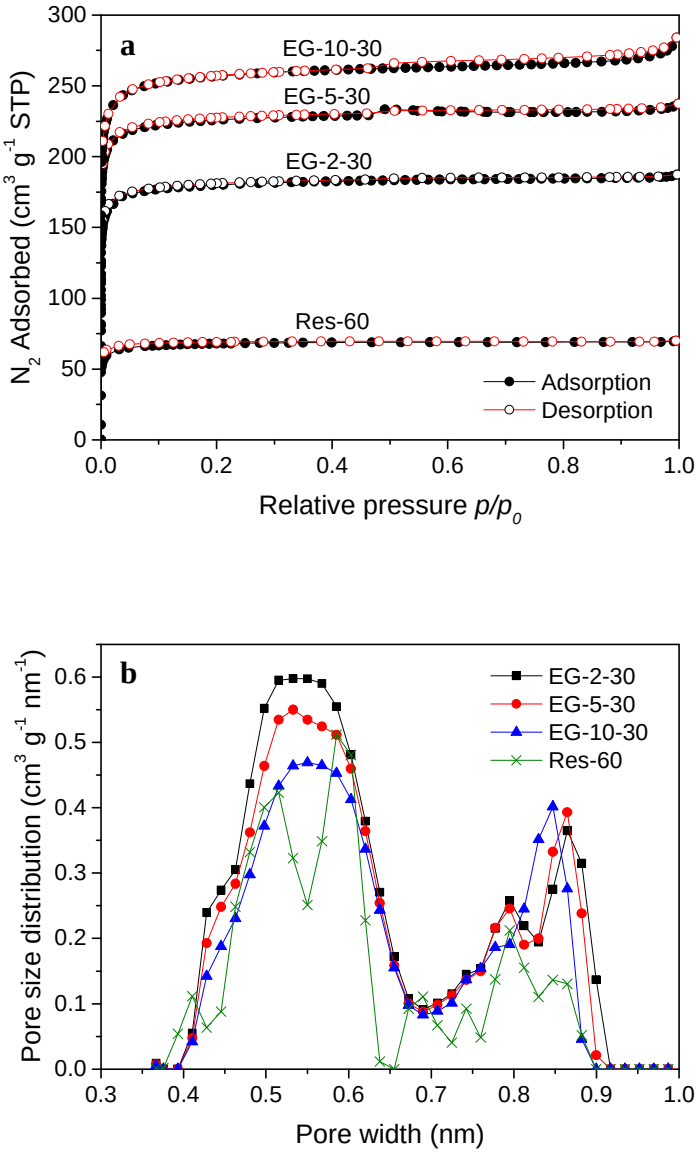

Fig. 3 (a) N_2 sorption isotherms at 77 K for the activated phenolic resin (Res-60) and the EG composites activated for 30 min and (b) their narrow micropore (< 1 nm) size distributions obtained from CO_2 adsorption at 273 K.

It is well established that adsorption of CO_2 on porous carbons under ambient temperature and pressure conditions is attributed to narrow micropores less than 1 nm.[23] Smaller micropore sizes below 0.8 and 0.7 nm have been reported to be responsible for CO_2 uptake at atmospheric pressure of 1 bar.[22,24,25] The

flue gas is typically only 10-15% CO_2, i.e. CO_2 partial pressure of 0.1-0.15 bar, which suggests that narrow micropores with a even smaller pore size contribute to CO_2 adsorption in PCC. Such ultra-narrow micropores are difficult to be detected due to slow diffusion of N_2 molecules at 77 K. In this regard, CO_2 physisorption at 273 K is more effective to obtain rapid high-resolution characterization of narrow micropores in carbons. For comparison, the narrow micropore (< 1 nm) size distribution (NMPSD) of ES-2-30 was obtained from both N_2 adsorption isotherm at 77 K (Fig. 3a) and CO_2 adsorption isotherm at 273 K (ESI Fig. S2), as presented in ESI Fig. S3. Compared to N_2 adsorption, features of the NMPSD are captured in much greater detail with the DFT calculation from CO_2 adsorption, and pore filling for ultra-small narrow micropores less than 0.5 nm can be observed from CO_2 adsorption.

Fig. 3b displays the NMPSDs of the activated phenolic resin and three EG composites obtained from CO_2 adsorption isotherms at 273 K (ESI Fig. S2). The corresponding surface areas (S_{nm}) and pore volumes (V_{nm}) of narrow micropores are listed in Table 1. It is evident that the EG composites have considerably enhanced development of narrow micropores compared to resin alone derived Res-60, exhibiting higher values of S_{nm} and V_{nm}. Among the three EG composites activated for 30 min, EG-2-30 contains the least amount of EG but exhibits the highest narrow microporosity in the pore size range below 0.7 nm. It is worth noting that only a small amount of EG addition (2%) to the phenolic resin can dramatically improve the narrow microporosity of the resultant carbon material.

The CO_2 equilibrium adsorption capacities at different CO_2 partial pressures were obtained from CO_2 adsorption isotherms at 298 K (Fig. 4). CO_2 molar capacity (mmol g^{-1}) was plotted in Fig. 4 whilst CO_2 mass (mg g^{-1}) capacity was listed in Table 1. The values of molar and mass capacity represent mmol and mg of CO_2 adsorbed per g of adsorbent, respectively. The CO_2 uptake at ambient saturated CO_2 pressure of 1 bar was denoted as C_{100}. As noted above, the content of CO_2 is low in the flue gas, so in practice CO_2 adsorption at a low CO_2 partial pressure is a more realistic measure of adsorbent

performance for PCC. The CO_2 uptake at 0.15 bar corresponding to 15% CO_2 partial pressure, denoted as C_{15}, was defined as an indicator of the low-pressure CO_2 adsorption capacity. Fig. 4 clearly shows that the EG composite possesses significantly enhanced CO_2 adsorption capacities compared to resin alone Res-60 at 298 K and over the measured pressure range up to 760 mmHg. The CO_2 uptake of the EG composite declines with an increased incorporation amount of EG. EG-2-30 exhibits the highest CO_2 uptake amongst the three EG composites activated for 30 min. The C_{100} of EG-2-30 (135 mg g^{-1}) is 65% higher than that of resin alone Res-60 (82 mg g^{-1}), while the improvement in the CO_2 uptake at the low pressure (C_{15}) is even more striking, increasing by 88% to 45 mg g^{-1} for EG-2-15 compared to 24 mg g^{-1} for Res-60 (Table1). In addition to greatly enhanced CO_2 adsorption capacity, sorption of CO_2 in the EG composite is reversible and no significant hysteresis in adsorption-desorption curves was observed (Fig. 4). This is desirable for recycle and regeneration of solid adsorbents after CO_2 capture.

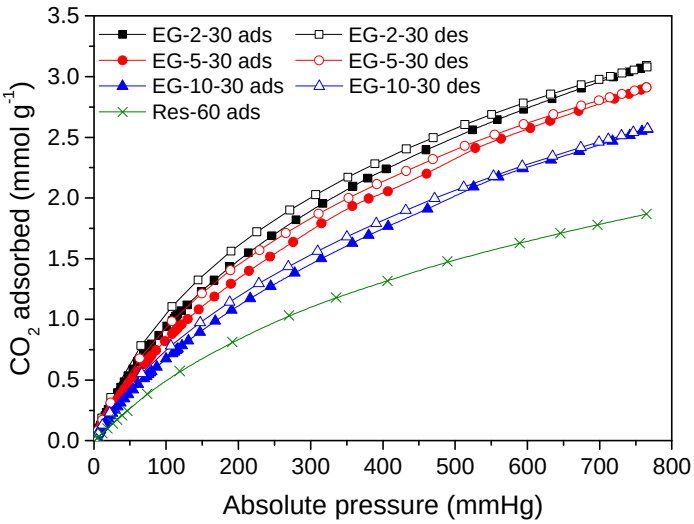

Fig. 4 CO_2 adsorption-desorption isotherms at 298 K for the EG composites activated at 950 ^oC for 30 min. The CO_2 adsorption isotherm of the activated phenolic resin (Res-60) at 298 K is plotted for comparison.

The above performance of CO_2 adsorption is in good agreement with the variation in NMPSDs of the adsorbents as revealed in Fig. 3b. The CO_2 uptake in the EG composite is remarkably improved compared to resin alone, which is attributed to a substantial improvement in the narrow microporosity with an incorporation of EG. For a given activation time of 30 min, the narrow microporosity (< 0.7 nm) of the EG composite responsible for CO_2 uptake at ambient conditions decreases in proportion to the EG content, thereby with EG-2-30 having the largest CO_2 uptake among the three EG composites. In addition, there are no correlations between the CO_2 uptake of the adsorbents and their textural properties other than characteristics of narrow micropores, such as surface areas S_{BET} and total pore volumes V_t. As listed in Table 1, the more EG the composite contains, the higher values are obtained for both S_{BET} and V_t. In contrast, the best CO_2 capacity was observed in EG-2-30 containing the least amount of EG.

Based on our previous study,[20] the extent of burn-off greatly influences the CO_2 capacity of CNT composite adsorbents prepared by CO_2 activation. To investigate this effect in the EG composite, we chose the best-performed EG composite containing 2% EG to be activated at 950 ^oC for 15 min, labeled as EG-2-15. The CO_2 adsorption isotherm of EG-2-15 at 298 K is shown in Fig. 5. Compared to EG-2-30, EG-2-15 has much lower burn-off of 7.6 wt%, but improved C_{15} at 4.7 mg g^{-1} and reduced C_{100} at 127 mg g^{-1} (Table 1). As shown in their NMPSDs (ESI Fig. S4), EG-2-15 has a larger proportion of micropores below 0.55 nm but less microporosity in the pore size range above 0.55 nm compared to EG-2-30. The variation of the NMPSD well elucidates the increase of C_{15} and decrease of C_{100} in EG-20-15. The extended activation widens narrow micropores, which may benefit CO_2 uptake at higher CO_2 pressures but deteriorate CO_2 adsorption at lower pressures. While the narrow micropore size range responsible for CO_2 adsorption at 298 K and various pressures cannot yet be defined exactly, it is clear from our results that the C_{15} value - the specific performance indicator of adsorbents in use for PCC - is most influenced by narrow micropores smaller than about 0.55 nm. This accords with the

observation that the CO_2 uptake at lower pressures purely depends on the fraction of fine micropores below 0.5 nm for phenolic resin derived activated carbon spheres prepared by KOH chemical activation.[22] In addition, with a same level of burn-off as resin alone Res-60, EG-2-15 has dramatically enhanced CO_2 uptake, particularly for C_{15} at 47 mg g^{-1} almost twice (96% increase) that of Res-60.

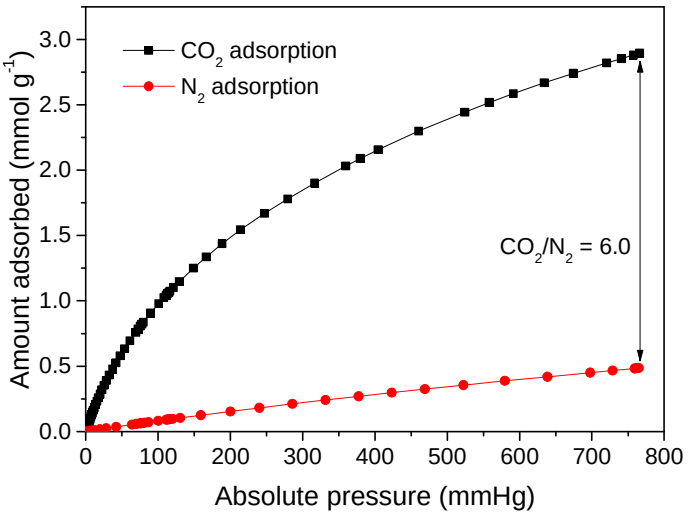

Fig. 5 CO_2 and N_2 adsorption isotherms of EG-2-15 at 298 K.

Values of up to 135 mg g^{-1} (3.07 mmol g^{-1}) and 47 mg g^{-1} (1.06 mmol g^{-1}) were achieved in the EG composites for C_{100} and C_{15}, respectively. They are lower than those of our previous CNT-incorporated phenolic resin-based composite carbons (maximum C_{100} at 159 mg g^{-1} and C_{15} at 52 mg g^{-1}). However, the EG composites outperform other phenolic resin-based activated carbons prepared with organic additives by CO_2 activation, in which the C_{100} up to 108 mg g^{-1} was obtained.[26] Moreover, indicative of CO_2 adsorption capacity under the flue gas condition, the C_{15} exhibited by the EG composite adsorbent is among the highest reported for porous carbons based on recently published comparisons (17-52 mg g^{-1} at 298 K and 0.15 bar).[20,27]

As the flue gas is comprised of around 80% nitrogen, a key PCC performance factor is the selectivity of the adsorbent for capturing CO_2 over N_2. A high CO_2/N_2 selectivity both increases the overall efficiency by boosting the CO_2 uptake, and results in a purer CO_2 capture product. CO_2 and N_2 adsorption capacities of EG-2-15 were compared at 298 K. As shown in Fig. 5, the amount of CO_2 adsorbed in EG-2-15 is much higher than that for N_2. Its equilibrium CO_2/N_2 adsorption ratio at 1 bar is 6.0 (2.89 mmol g^{-1} CO_2 vs. 0.48 mmol g^{-1} N_2), close to the ratio 6.3 of our composite with CNTs.[20] This value is even superior to those of porous carbons prepared by KOH activation from petroleum pitch (2.8),[28] petroleum coke (5.1)[29] and sawdust-based chars (5.4).[10] In addition, CO_2 and N_2 adsorption isotherms at 298 K for other three EG composites activated for 30 min were also compared (Fig. S5). With an increase of EG content, the CO_2 uptake is decreased and the amount of N_2 adsorbed is also slightly reduced with the N_2 uptake at 1 bar being 0.49, 0.47 and 0.41 mmol g^{-1}, respectively for EG-2-30, EG-5-30 and EG-10-30. Similar to that of EG-2-15, the equilibrium CO_2/N_2 adsorption ratios at 1 bar are around 6.2-6.3 for the above three EG composites.

We also calculated the CO_2/N_2 adsorption selectivity at 298 K using the ratio of the initial slopes of CO_2 and N_2 adsorption isotherms at very low pressures (ESI Fig. S6). EG-2-15 has a high initial selectivity of 18.1. This is comparable to that of the CNT composite (19.8),[20] substantially better than reported for pristine microporous carbons (~7)[30,31] and N-doped microporous carbons based on polyimine (12.5)[32] and even better than graphene-polyaniline composites (17.9).[33] However, the carbon-based adsorbents generally show much lower CO_2/N_2 adsorption selectivities than recently reported microporous polymer adsorbents such as microporous polyaminals (104)[34] and microporous polyimides (56)[35]. Such remarkable CO_2/N_2 selectivities are attributed to the abundant CO_2-philic functional groups in the microporous polymer in addition to the contribution from the microporous structure.

To understand the affinity of the EG composite to CO_2 molecules, the isosteric heat of CO_2 adsorption for EG-2-15 was calculated from isotherms at 273, 298 and 323 K (ESI Fig. S7). It is obvious that the CO_2 uptake is decreased with an increase of adsorption temperature, which is consistent with the physisorption nature for CO_2 adsorption on pristine microporous carbons. At 323 K, the values of C_{15} and C_{100} for EG-2-15 are reduced to 32 and 107 mg g^{-1}, respectively. At near zero CO_2 loading the isosteric heat is 31.0 kJ mol^{-1} and declines to 22.4 kJ mol^{-1} at 2 mmol g^{-1} of CO_2 adsorbed (Fig 6). The value for EG-2-15 (31.0 kJ mol^{-1}) is slightly lower than that of the CNT composite (32.6 kJ mol^{-1}),[20] but higher than for N-free pristine porous carbons (20-30 kJ mol^{-1}).[10,36] The heat of adsorption at low surface coverage indicates the interaction between the adsorbent and adsorptive molecules, relying on the pore size distribution in the case of CO_2 physisorption on pristine porous carbons by considering the fact that smaller micropores engender stronger interactions between CO_2 molecules and porous carbons than larger micropores. Hence, the high heat of CO_2 adsorption for EG-2-15 should be attributed to its well-developed narrow microporosity.

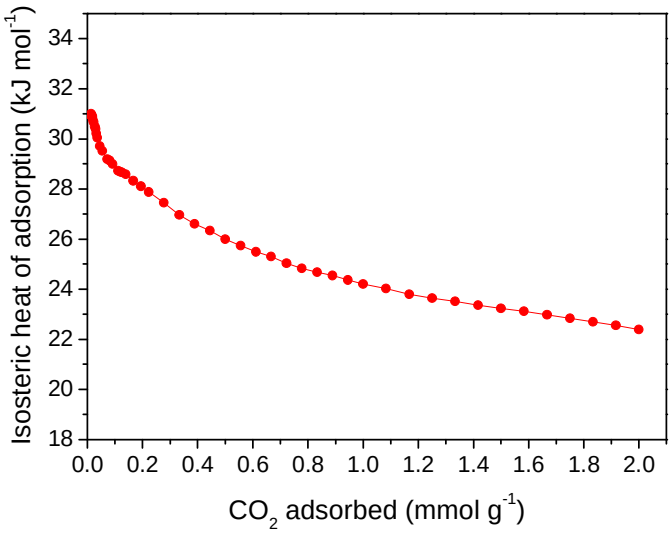

Fig. 6 Isosteric heat of CO_2 adsorption for EG-2-15.

4. Conclusions

The addition of a small proportion of EG to the phenolic resin dramatically hastens the CO_2 activation and improves the development of microporous structures in resin-derived activated carbons. The resultant EG composite carbons exhibit large pore surface areas and volumes more than three times higher than for resin alone. The narrow microporosity responsible for the CO_2 uptake at ambient conditions is also remarkably enhanced with the inclusion of EG. The improvement of CO_2 uptake in the EG composites is striking with an increase of up to 65% and 96% for C_{100} and C_{15}, respectively. The EG composites have lower CO_2 adsorption capacities than our previous CNT composite carbons but outperform other reported phenolic resin based activated carbons. In particular, they show superior CO_2 uptake at low pressures, which is more important to PCC applications. The EG composite adsorbent exhibits excellent CO_2/N_2 selectivity of 18.1 at 298 K, and a strong affinity to CO_2 molecules indicated by its high heat of CO_2 adsorption (31.0 kJ mol^{-1}).

In addition to their superior CO_2 adsorption properties, the physically activated EG composite adsorbents are especially attractive as the EG component is inexpensive, available in very large amounts and easy to handle and is only required at a low addition level of around 2 wt%. The EG component dramatically reduces the activation time and the extent of burn-off necessary to give an excellent PCC adsorbent. This greatly reduces the energy required to produce the adsorbent and the waste generated in activation and further enhances its cost and environmental advantages over chemical activation and functionalization of porous carbons. Therefore, the newly developed EG composite carbon adsorbents are promising for large-scale deployment and commercial applications to PCC.

Acknowledgements

This research was funded by CSIRO. The expandable Graphite (Grade 3772) was donated by Asbury Carbons.

References

1 D. M. D'Alessandro, B. Smit and J. R. Long, *Angew. Chem. Int. Ed.*, 2010, **49**, 6058-6082.

2 Q. Wang, J. Luo, Z. Zhong and A. Borgna, *Energy Environ. Sci.*, 2011, **4**, 42-55.

3 A. Samanta, A. Zhao, G. K. H. Shimizu, P. Sarkar and R. Gupta, *Ind. Eng. Chem. Res.*, 2012, **51**, 1438-1463.

4 S. Choi, J. H. Drese and C. W. Jones, *ChemSusChem*, 2009, **2**, 796-854.

5 Y. F. Zhao, X. Liu and Y. Han, *RSC Adv.*, 2015, **5**, 30310-30330.

6 Z.H. Chen, S.B. Deng, H.R. Wei, B. Wang, J. Huang and G. Yu, *Front. Environ. Sci. Eng.*, 2013, **7**, 326-340.

7 J. Liu, P. K. Thallapally, B. P. McGrail, D. R. Brown and J. Liu, *Chem. Soc. Rev.*, 2012, **41**, 2308-2322.

8 F. A. Hasan, P. Xiao, R. K. Singh and P. A. Webley, *Chem. Eng. J.*, 2013, **223**, 48-58.

9 X.Y. Ma, Y. Li, M. H. Cao and C. W. Hu, *J. Mater. Chem. A*, 2014, **2**, 4819-4826.

10 M. Sevilla and A. B. Fuertes, *Energy Environ. Sci.*, 2011, **4**, 1765-1711.

11 G. P. Hao, W. C. Li and A. H. Lu, *J. Mater. Chem.*, 2011, **21**, 6447-6451.

12 Z. J. Zhang, Z. Z. Yao, S. C. Xiang and B. L. Chen, *Energy Environ. Sci.*, 2014, **7**, 2868-2899.

13 P. Mohanty, L. D. Kull and K. Landskron, *Nat. Commun.*, 2011, **2**, 401.

14 L. K. C. de Souza, N. P. Wickramaratne, A. S. Ello, M. J. F. Costa, C. F. da Costa and M. Jaroniec, *Carbon*, 2013, **65**, 334-340.

15 J. C. Wang, A. Heerwig, M. R. Lohe, M. Oschatz, L. Borchardt, and S. Kaskel, *J. Mater. Chem.*, 2012, **22**, 13911-13913.

16 G. P. Hao, W. C. Li, D. Qian and A. H. Lu, *Adv. Mater.*, 2010, **22**, 853-857.

17 L. Zhao, Z. Bacsik, N. Hedin, W. Wei, Y. H. Sun, M. Antonietti and M. M. Titiric, *ChemSusChem*, 2010, , 840-845.

18 M. Nandi, K. Okada, A. Dutta, A. Bhaumik, J. Maruyama, D. Derks and H. Uyama, *Chem. Commun.*, 2012, **48**, 10283-10285.

19 S. R. Tennison, *Appl. Catal. A: General*, 1998, **173**, 289–311.

20 Y. G. Jin, S. C. Hawkins, C. P. Huynh and S. Su, *Energy Environ. Sci.*, 2013, **6**, 2591-2596.

21 T.F. Liu, L. Zhao, J.S. Zhu, B. Wang, C.F. Guo and D.L. Wang, *J. Mater. Chem. A*, 2014, **2**, 2822-2829.

22 N. P. Wickramaratne and M. Jaroniec, *J. Mater. Chem. A*, 2013, **1**, 112-116.

23 Z. Zhang, J. Zhou, W. Xing, Q. Xue, Z. Yan, S. Zhuo and S. Z. Qiao, *Phys. Chem. Chem. Phys.*, 2013, **15**, 2523-2529.

24 V. Presser, J. McDonough, S. H. Yeon and Y. Gogotsi, *Energy Environ. Sci.*, 2011, **4**, 3059-3066.

25 J. P. Marco-Lozar, M. Kunowsky, F. Suárez-García and A. Linares-Solano, *Carbon*, 2014, **72**, 125-134.

26 C. F. Martin, M. G. Plaza, S. Garćia, J. J. Pis, F. Rubiera and C. Pevida, *Fuel*, 2011, **90**, 2064-2072.

27 A. S. González, M. G. Plaza, F. Rubiera and C. Pevida, *Chem. Eng. J.*, 2013, **230**, 456-465.

28 A. Wahby, J. M. Ramos-Fernandez, M. Martinez-Escandell, A. Sepulveda-Escribano, J. Silvestre-Albero and F. Rodriguez-Reinoso, *ChemSusChem*, 2010, **3**, 974-981.

29 X. Hu, M. Radosz, K. A. Cychosz and M. Thommes, *Environ. Sci. Technol.*, 2011, **45**, 7068-7074.

30 J. D. Carruthers, M. A. Petruska, E. A. Sturm and S. M. Wilson, *Microporous Mesoporous Mater.*, 2012, **154**, 62-67.

31 C. Ducrot-Boisgontier, J. Parmentier, A. Faour, J. Patarin and G. D. Pirngruber, *Energy Fuels*, 2010, **24**, 3595-3602.

32 J. C. Wang, I. Senkovska, M. Oschatz, M. R. Lohe, L. Borchardt, A. Heerwig, Q. Liu and S. Kaskel, *J. Mater. Chem. A*, 2013, **1**, 10951-10961.

33 K. C. Kemp, V. Chandra, M. Saleh and K.S. Kim, *Nanotechnology*, 2013, **24**, 235703-235710.

34 G. Y. Li, B. Zhang, J. Yuan and Z. G. Wang, *Macromolecules*, 2014, **47**, 6664-6670.

35 C. J. Shen and Z. G. Wang, *J. Phys. Chem. C*, 2014, **118**, 17585-17593.

36 S. Himeno, T. Komatsu and S. Fujita, *J. Chem. Eng. Data*, 2005, **50**, 369-376.